مجلة جامعة بني وليد للعلوم الإنسانية والتطبيقية
Bani Waleed University Journal of Humanities and Applied Sciences
تصدر عن– جامعة بني وليد – ليبيا
Website:https://jhas-bwu.com/index.php/bwjhas/index
ISSN 3005-3900 الصفحات (233 -260) المجلد الحادي عشر ــ العدد الثالث ــ 2026

Structural and electronic modulation of TiO_2/Tiopronin hybrid nanoparticles: correlation with antibacterial activity under sunlight

Rasha Shakir Mahmood*[1], Suhad Yassein Abed [2], Dhia Hadi Hussain [3], Mohamad Faraj Al-Marjani[2]

[1]Department of Chemistry, College of Science, Mustansiriyah University, Baghdad, Iraq.
[2.4] Department of Biology, College of Science, Mustansiriyah University, Baghdad, Iraq.
[3]Department of Medical Physics, College of Science, Al-Esraa University, Baghdad, Iraq.
rashashakir.m@uomustansiriyah.edu.iq

التعديل الهيكلي والإلكتروني للجسيمات النانوية الهجينةTiO_2 / Tiopronin : العلاقة مع الفعالية المضادة للبكتيريا تحت ضوء الشمس

رشا شاكر محمود [1]*، سهاد ياسين عبد [2]، ضياء هادي حسين [3]، محمد فرج شذر [4]
[1] قسم الكيمياء، كلية العلوم، الجامعة المستنصرية، بغداد، العراق.
[4.2] قسم الأحياء، كلية العلوم، الجامعة المستنصرية، بغداد، العراق.
[3] قسم الفيزياء الطبية، كلية العلوم، جامعة الإسراء، بغداد، العراق.

Received: 25-03-2026	Accepted: 07-05-2026	Published: 15-05-2026

الملخص:

في هذه الدراسة تم تحضير جسيمات نانوية من TiO_2 و(TiO_2/Tiopronin) بواسطة طريقة القصف بالليزر. تم فحص الجسيمات النانوية باستخدام المجهر الالكتروني النافذ (TEM)، المجهر الإلكتروني الماسح للانبعاث الميداني (FE-SEM)، حيود الاشعة السينية (XRD). أظهرت نتائج حيود الاشعة السينية ان حجم الجسيمات النانوية لـ TiO_2 صغيرة جداً تصل الى (20.17) نانومتر بينما حجم الجسيمات النانوية لـ (TiO_2/Tiopronin) يصل لـ (53) نانومتر وهذا يعتبر اصغر قطر تم الحصول علية بهذه الطريقة. في المقابل أظهرت نتائج (TEM) ان حجم الجسيمات النانوية لـ TiO_2 بلغ (17) نانومتر وحجم الجسيمات النانوية لـ (TiO_2/Tiopronin) بلغ (49) نانومتر. في هذا العمل درسنا تأثير ضوء الشمس مع الجسيمات النانوية لـ TiO_2 و الجسيمات النانوية لـ (TiO_2/Tiopronin) على البكتيريا *Pseudomonas Aeruginosa* المعزولة من التهابات الحروق، ولاحظنا أن الجسيمات النانوية (TiO_2/Tiopronin) أظهرت تثبيطًا أكبر لنمو بكتيريا *Pseudomonas Aeruginosa* مقارنةً بالتثبيط الناتج عن ضوء الشمس والدقائق النانوية لـ TiO_2 منفردة. لذا، يمكننا القول أننا نجحنا في تحضير جسيمات نانوية مفيدة (TiO_2/Tiopronin) باستخدام طريقة خضراء بسيطة بأقل كلفة واستخدامها لتثبيط بكتيريا *Pseudomonas Aeruginosa* التي تسبب التهابات الحروق.

الكلمات الدالة: جسيمات نانوية TiO2، جسيمات نانوية TiO2/Tiopronin، التحفيز الضوئي، القصف بالليزر، بكتيريا Pesudomonas Areuginosa

Abstract

In this study, we prepared TiO_2 nanoparticles and nanoparticles (TiO_2/Tiopronin) by Laser ablation. The nanoparticles were measured using transmission Electron Microscopy (TEM), Field emission

scanning electron microscopy (FE-SEM), and x-ray diffraction (XRD). the results of X-Ray diffraction show that TiO_2 nanoparticles have a very small size reached (20.17) nm while the nanoparticles (TiO_2/Tiopronin) have (53) nm and this consider the lowest diameter obtained in this method while the results by TEM showed the size of TiO_2 nanoparticles is (17) nm and the size of the nanoparticles (TiO_2/Tiopronin) is (49) nm, in this work, we studied the effect of the sunlight with TiO_2 nanoparticles and nanoparticles (TiO_2/Tiopronin) on *Pseudomonas Aeruginosa* isolated from burn infections and we noticed that the nanoparticles appear a higher inhibition towards the *Pseudomonas Aeruginosa* more than the inhibition by sunlight and TiO_2 nanoparticles alone. So, we can say that we succeeded in preparing useful nanoparticles (TiO_2/Tiopronin) by using a simple green method with the lowest cost and using it to inhibit the *Pseudomonas Aeruginosa* that cause Burn Infections.

Keywords: TiO_2 nanoparticles, Titanium/Tiopronin, nanoparticles, Photocatalysis, Liquid laser ablation, Pseudomonas Aeruginosa.

Introduction

Recently, the interest of scientists and researchers in the so-called nanotechnology and nanomaterials has increased, which has become involved in many fields, especially the medical field, the field of drug delivery and treatment of cancer diseases, and many other applications that directly affected our lives as living humans on the ground and this basis, it has become necessary to shed light on the most important nanomaterials that have become widely used in this technology, namely, metals and metal oxides such as silver, gold, copper, nickel, cadmium, zinc, and others[1-3]. perhaps one of the most important metal oxides that have been widely used in nanotechnology in the field of medicine, cosmetics, dyes, the manufacture of solar cells and sensors are all phases of TiO_2 nanoparticles, their importance is due to their distinctive and unique properties [4,5] They are a white powder that is characterized as a non-toxic, which means that it can be classified as environmentally friendly and human-friendly [6]. In addition to the stability characters at high temperatures and the high surface area per volume, which gives possibility to use as a very effective photo-catalyst when exposed to ultraviolet rays, with a very high ability to break down organic pollutants and convert them into other forms that are friendly to the environment and humans [7,8]. It should be noted that titanium dioxide nanoparticles (TiO_2) NPs exist in three forms, namely anatase, rutile, and brookite, and each of these forms has its own bandgap energy. Rutile is 3 eV while anatase 3.2 eV [9]. In general, nanomaterials are prepared in many ways, including chemical, physical and biological methods but recently has become a Pulsed laser ablation technique of the most important techniques used in the production of nanomaterials because of the possibility of obtaining directly the nanoparticles in liquids and avoid the use of electrical equipment and low cost of production in addition to the simplicity and the absence of contamination and get many kinds of colloidal nanoparticles [10,11]. Prior studies have demonstrated that laser-synthesized TiO_2 NPs have significant antibacterial activity, despite the fact that their efficacy is heavily influenced by particle size, irradiation conditions, and surface modification. According to Khashan et al. (2021), TiO_2 NPs (20–30 nm) produced by laser ablation showed concentration-dependent antibacterial activity against both Gram-positive and Gram-negative bacteria, with increased inhibition under UV irradiation due to the production of reactive oxygen species (ROS) [12]. When Haleem et al. (2018) synthesized TiO_2 NPs (30–100 nm) using laser ablation, they observed sturdy antimicrobial outcomes, which they attributed to the excessive purity and surface reactivity of laser-generated nanoparticles [13]. Furthermore, Dell'Aglio et al. (2014) tested that once exposed to UV light, laser-ablated TiO_2 NPs 34 nm exhibited extra antibacterial and photocatalytic interest, specifically due to efficient electron–hole separation and oxidative

radical formation [14]. More lately, Haji et al. (2024) stated strong antibacterial and antibiofilm interest of TiO_2 NPs towards multidrug-resistant Pseudomonas aeruginosa, confirming membrane harm and structural disruption of bacterial cells as the main mechanism of movement [15]. Furthermore, TiO_2/ZnO nanoparticless confirmed higher antibacterial overall performance than single metallic oxides (Faisal et al., 2020), highlighting the critical role that compositional change plays in improving ROS manufacturing and fee switch efficiency [16]. Tiopronin is a natural compound; its structure is $C_5H_9NO_3S$, a medicinal agent usually used for systemic situations which include cystinuria and Wilson's disorder. According to certain research, Tiopronin's capability to inhibit the increase of commonplace micro-organism like E. Coli and prevent the formation of biofilms has been superior with the aid of chemical changes brought approximately by using blending it with other substances [17].

This work presents the first report on the fabrication of TiO_2/Tiopronin organic–inorganic hybrid nanoparticles via a clean laser ablation route, demonstrating significantly enhanced sunlight-driven antibacterial performance through bandgap modulation, improved charge separation, and dominant hydroxyl radical-mediated ROS generation.

2. Materials and Methods

In this study, used Ti plate (purity 99.99% from Sigma Aldrich, Germany), Chloroform ($CHCl_3$) (99.99% from Appli-chem, Germany), Ethanol (C_2H_5OH) (purity 99.99% from Sigma- Aldrich, Germany), Acetic acid ($C_2H_4O_2$).

2.1. Preparation of TiO_2 NPs

TiO_2 NPs were created using the straightforward pulsed laser ablation in liquid (LAL) method as illustrated in (Fig.1). To remove surface impurities, a titanium metal plate measuring 3 × 3 cm^2 and 1 mm in thickness was ultrasonically cleaned in chloroform, ethanol, and deionized (DI) water for 15 minutes each. It was then dried at room temperature and fixed at the bottom of a beaker filled with 15 mL of ethanol and acetic acid (1:1). The ablation source was an Nd:YAG laser operating at 1064 nm wavelength, 10 ns pulse duration, 10 Hz repetition rate, and 80 mJ pulse energy. The target surface was carefully positioned at the focal plane 8.5 cm from the lens, and the laser beam was focused onto the target using a convex lens with a focal length of 8 cm. The ablation procedure was run at room temperature (30°C) for 12 minutes. After that, the colloidal suspension was left to stabilize at room temperature. then collected by centrifugation at 4000 rpm for 50 minutes, then cleaned with DI to get rid of any impurities, and finally dried using a vacuum oven at 60°C for 15 hours. For structural analysis and antibacterial experiments, the experiment was conducted several times in order to obtain a sufficient yield [18].

2.2. Prepararion TiO_2 / Tiopronin Nanoparticles

The same method used to prepare TiO_2 NPs was used to create TiO_2 nanoparticles coated with Tiopronin, but a different solution was used (0.4) g of Tiopronin was dissolved in ethanol and DI with acetic acid (1:1:1) as illustrated in (Fig.1).

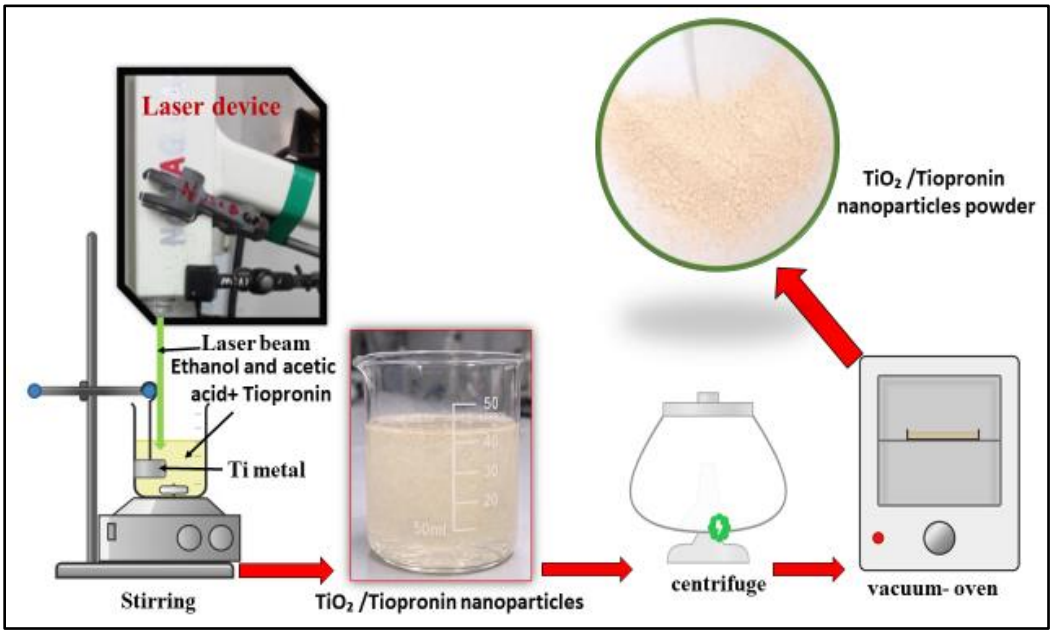

Fig .1 Synthesis TiO_2 NPs and TiO_2/Tiopronin nanoparticles by LAL method.

2.3. Pathogenic Bacteria

Isolates of *Pseudomonas aeruginosa* were obtained from Department of Biology/College of Science/ Mustansiriyah University/Baghdad / Iraq.

2.4. Preparation of culture medium and bacterial suspension with nanomaterials

both nanomaterials that synthesized by laser ablation were screened for their antibacterial effect against pathogenic bacteria using co - culture technique. The bacterial culture of pathogenic bacteria was grown in nutrient broth with a ratio (1:1) (TiO_2 NPs solution: nutrient broth) and (TiO_2/Tiopronin nanoparticles solution: nutrient broth), we used different concentrations of TiO_2 NPs and TiO_2/Tiopronin nanoparticles (0.2-1 mg/mL) and the control medium contained nutrient broth only [19], Co-cultures and control were incubated at 37℃ for 24 h, After the incubation 1mL of each culture was serially diluted up to 10^{-1} to 10^{-6}, Then 0.1mL of 10^{-6} dilution sample was taken and spread on nutrient agar plates. The plates were incubated at 37 ℃ for 24 h. The colonies were counted and the inhibition activity was evaluated after 24 h and calculated percent reduction of bacteria using the following equation described as Ghosh et al. [20]:

$$R(\%) = \frac{(A-B)}{A} \times 100 \text{ …….. (1)}$$

Where **R** is the reduction rate, **A** is the number of bacterial colonies from the control medium, and **B** is the number of bacterial colonies treated with TiO_2 NPs.

3. Antibacterial activity of synthesized nanoparticles with Sunlight

Both solutions (bacterial culture and the controlling medium) were placed in an incubator at a temperature of 37^{o}C for 24 h. After the incubation process, (1 mL) of both solutions were taken. Several dishes containing the bacterial culture samples were prepared, then each dish was treated separately. Where the dish containing the bacterial culture was exposed only to sunlight for different periods of time ranging from (1 -5) hours after which the sample was also incubated for 24 h after which the results were observed and the bacterial colonies were counted, and the second dish was The suspension of TiO_2 NPs with different concentrations (0.2-1) mg/mL was prepared by suspending them in distilled water and the solution was sonicated for 10 minutes to get the homogenous suspension, these nanoparticles of TiO_2 NPs uncoated with Tiopronin were added for bacterial culture and then the sample was exposed to the sunlight for different periods of time ranging from (1-5) hours after which the sample was also incubated for 24 h after which the results were observed and the bacterial colonies were counted, to study the bacterial concentration, Then the same experiment was repeated for the third dish, but by adding TiO_2 coated with Tiopronin (TiO_2/Tiopronin) nanoparticles, the number of colonies was counted and the inhibition activity was evaluated after 24 h by using the Ghosh equation [20, 21].

4. Results and discussion

4.1. Materials characterizations

The (LAL) was used to prepare TiO_2 NPs and TiO_2 / Tiopronin nanoparticles. The distinguishing feature of this technique is the quality of the product. The quality here is the trend towards increasing the percentage of small nanoparticles by diameter relative to the total number of prepared nanoparticles. All the samples in this study were analyzed using different techniques, like X-ray diffraction (XRD) (Malvern Panalytical device), field-emission scanning electron microscopy (FE-SEM) (Inspect F50 device), (Shimadzu FTIR-8400S) Fourier Transform Infrared Spectrophotometer (FTIR), transmission electron microscopy (TEM) (Thermo Fisher Scientific device), and The optical characteristics of TiO_2 NPs and TiO_2/Tiopronin nanoparticles were investigated at room temperature using UV-visible absorption spectroscopy (Shimadzu UV-2600) and photoluminescence (PL) spectroscopy (Horiba Fluorolog-3).

4.2. XRD of TiO_2 NPs and TiO_2/ Tiopronin nanoparticles

X-ray diffraction used to determine the crystalline shape as well as to identify the prepared nanoparticles. The characteristics of a continuous size model (step size of 2Ɵ = 0.05 deg) and at a speed of 5 deg./min), The processed voltages for the x-ray tube were 40 kV and the tube current (30 mA). X-ray was generated using a copper objective and the wavelength of the x-ray was generated (1.54 Å). The findings indicate that we had two different kinds of nanoparticles: the first one is TiO_2 NPs, as seen in (Fig.2) and (Table 1). where It is suggested that a pure phase with no observable impurity peaks has been established because every diffraction peak in the pattern agrees well with the standard data for crystalline TiO_2 NPs type anatase (JCPDS card no. 021-1272) [22]. Accordingly, the principal diffraction peaks of TiO_2 are 2θ = 25.4954°, 37.8335°, 48.2065°, 54.1268°, 55.3320°, 62.9599°, 68.9684°, 70.3113°, and 75.2268°. these values correspond to the planes (101), (004), (200), (105), (211), (204), (116), (220), and (215).

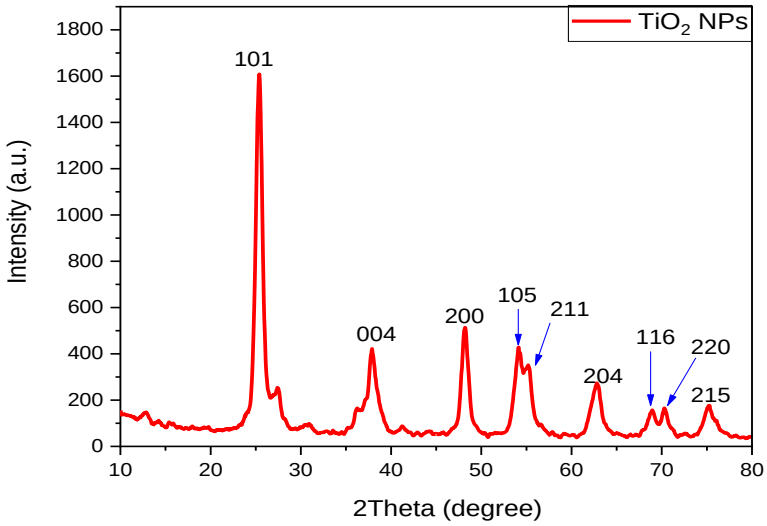

Fig.2 X-ray pattern of TiO_2 nanoparticles

Table 1 illustrate the data of XRD for TiO_2 NPS.

Pos. [°2Th.]	Height [cts]	FWHM Left [°2Th.]	d-spacing [Å]	Rel. Int. [%]	Tip Width
25.4954	1583.23	0.3936	3.49380	100.00	0.4723
37.8335	368.42	0.4920	2.37801	23.27	0.5904
48.2065	494.31	0.6888	1.88778	31.22	0.8266
54.1268	367.38	0.4920	1.69446	23.20	0.5904
55.3320	300.88	0.3936	1.66037	19.00	0.4723
62.9599	228.88	0.7872	1.47632	14.46	0.9446
68.9684	114.39	0.7872	1.36165	7.23	0.9446
70.3113	119.07	0.5904	1.33890	7.52	0.7085
75.2268	139.04	0.6888	1.26315	8.78	0.8266

And the second one is the TIO_2/Tiopronin nanoparticles. The principal diffraction peaks of TiO_2 NPs are clearly visible in (Fig.3) and (Table 2) at 2θ = 25.4954°, 37.8335°, 48.2065°, 54.1268°, 55.3320°, 62.9599°, 68.9684°, 70.3113°, and 75.2268°. These values correspond to planes (101), (004), (200), (105), (211), (204), (116), (220), and (215) [22]. Notably, we observe a decrease in the intensity of the TiO_2 peaks, indicating that an amorphous layer of Tiopronin is present on the TiO_2 NPs surface. Additionally, we observe from (Fig.3) that the presence of Tiopronin

caused broad peaks to appear in the range 11.7447°- 24.6501°. The amorphous nature of Tiopronin influences peak intensity, making the broad peak appear weak.

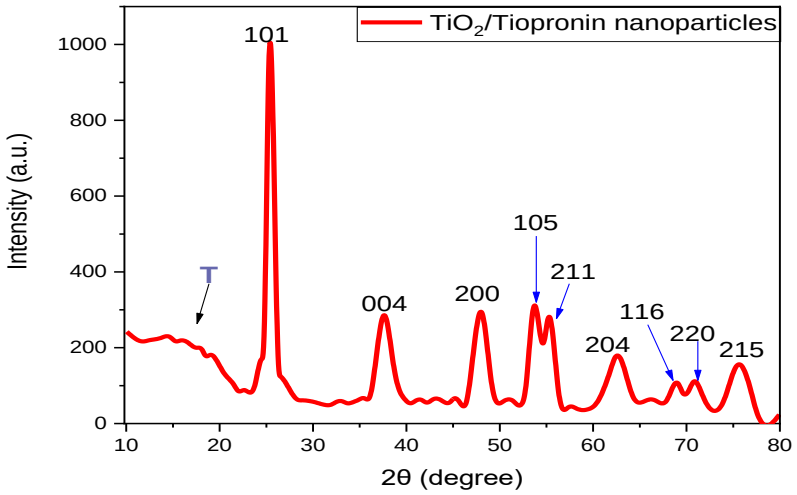

Fig.3 X-ray pattern of TiO_2 / Tiopronin nanoparticles.

Table 2 illustrate the data of XRD for TiO_2/Tiopronin.

Pos. [°2Th.]	Height [cts]	FWHM Left [°2Th.]	d-spacing [Å]	Rel. Int. [%]	Tip Width
11.7447	67.36	3.1488	7.53511	10.25	3.7786
24.6501	1375.19	0.2460	3.61167	68.57	0.2952
25.5025	657.23	0.6396	3.49284	100.00	0.7675
37.7457	262.99	0.5904	2.38334	40.02	0.7085
48.0203	409.56	0.7872	1.89467	62.31	0.9446
53.8885	306.63	0.6888	1.70138	46.66	0.8266
54.8875	291.89	0.6888	1.67276	44.41	0.8266
62.5549	236.60	0.6888	1.48491	36.00	0.8266
68.5084	81.43	0.7872	1.36966	12.39	0.9446
70.2220	104.01	0.7872	1.34038	15.83	0.9446
75.1380	165.50	0.6888	1.26442	25.18	0.8266

The results of the X-ray diffraction measurements, proved that these particles are nanoparticles and by the usage of the Scherrer equation [23]:

$$D = 0.9\,\lambda / \beta\, COS\,\Theta \quad \ldots\ldots\ldots\ldots\ldots\ldots (2)$$

Where **D** is the crystalline size, **λ** is the wavelength used, **β** shows the highest peak from the middle or Θ at the angle of diffraction of the peak. By applying this equation, the average crystalline size (20.17) nm was found for TiO_2 NPs only, while the average crystalline size of the TiO_2/Tiopronin nanoparticles was (53.80) nm.

4.3. FE-SEM of TiO_2 NPs and TiO_2/ Tiopronin nanoparticles

(Fig.4 **A, B**) shows the FE-SEM of the prepared TiO_2 NPs and TiO_2/Tiopronin nanoparticles, respectively. The form of the TiO_2 NPs appears slightly agglomerated due to van der Waals forces and high surface energy; the measured average particle size was found to be 19.34 nm. The particles' relatively uniform size and shape show that the preparation methods used were perfect.

On the other hand, because of the strong van der Waals forces and high surface energy of both TiO_2 NPs and Tiopronin, the TiO_2/Tiopronin nanoparticles appear as regular particles with slightly agglomerated. An average particle size of 50 nm was found.

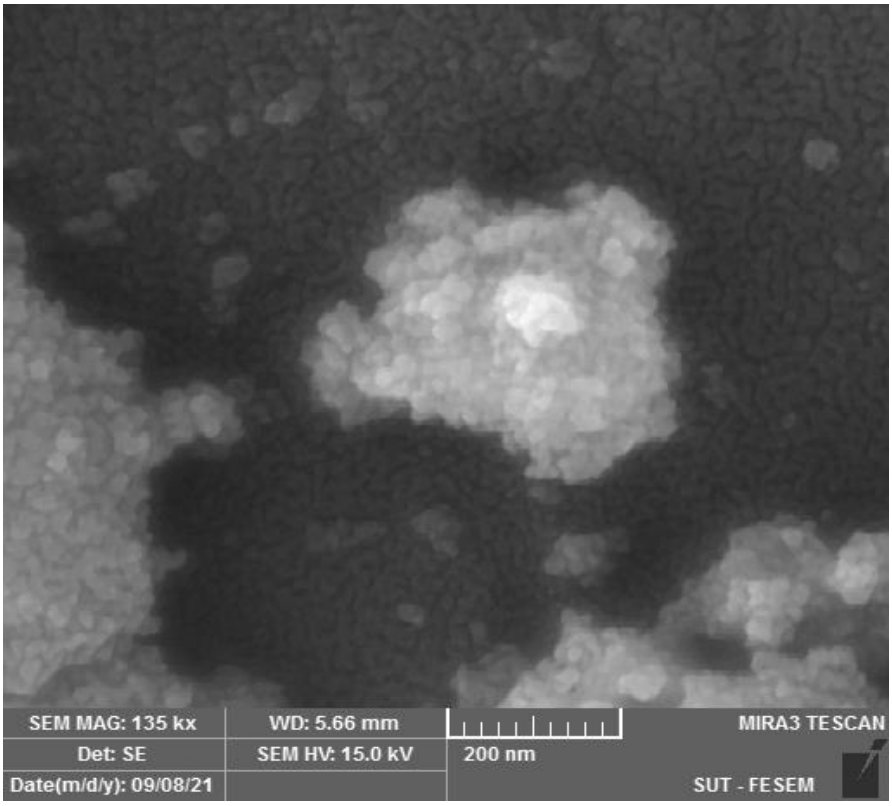

(A)

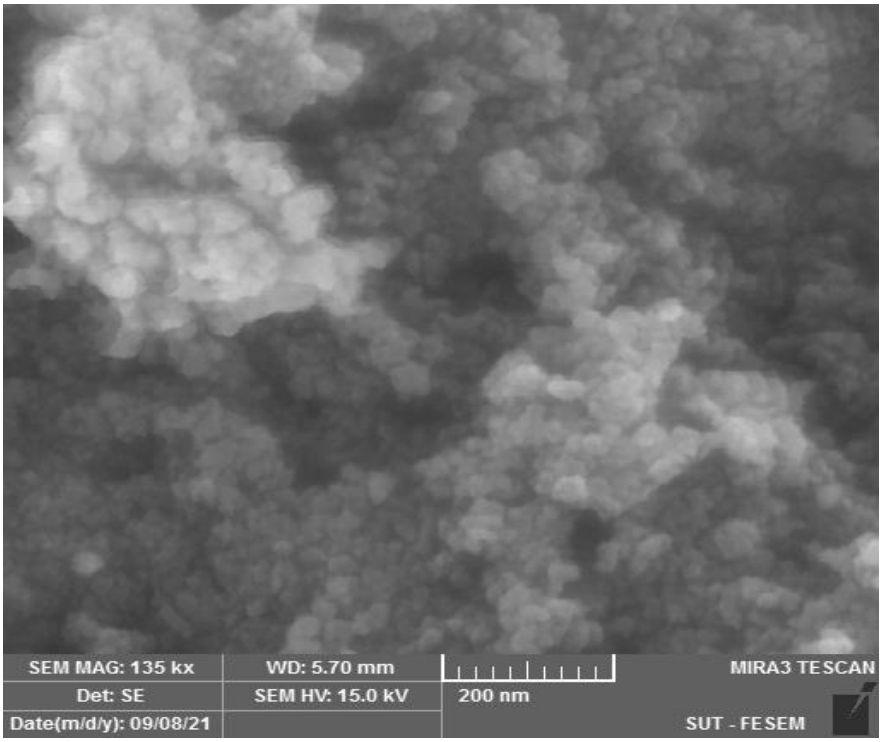

(B)

Fig.4 FE-SEM of **A** TiO_2 NPs, **B** FE-SEM of TiO_2 /Tiopronin nanoparticles prepared by laser ablation.

4.4. Energy-dispersive X-ray spectroscopy (EDS) of TiO_2 NPs and TiO_2/Tiopronin nanoparticles

This analysis was usually used to know the elemental composition of the synthesized TiO_2 NPs, where no signals corresponding to other elements or impurities were found in the spectrum; only titanium (Ti) and oxygen (O) were identified, as shown in (Fig.5A). In contrast, in (Fig.5B) we can see only carbon (C), sulfer (S), titanium (Ti), and oxygen (O) elements in the TiO_2/Tiopronin nanoparticles without any impurities, and this indicates the clean synthesis of all nanomaterials. It is important to note that the gold (Au) signals do not represent contamination; rather, they are a result of the gold coating that was applied to the sample to boost conductivity during FE-SEM analysis.

On the other hand, (Fig. 5C- H) shows the elemental mapping for TiO_2 NPs and TiO_2/Tiopronin nanoparticles, respectively, which shows that Titanium and Oxygen are the main elements in the synthesized TiO_2 NPs, and a large amount of carbon, which indicates the presence of Tiopronin in the TiO_2/Tiopronin nanoparticles.

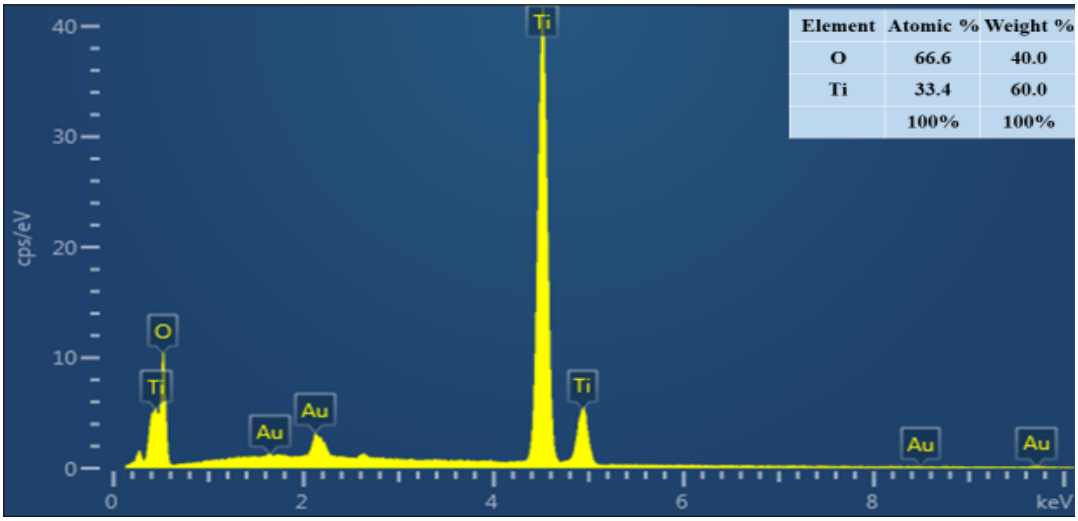
Element Atomic % Weight %
O 66.6 40.0
Ti 33.4 60.0
100% 100%
cps/eV
keV
O
Ti
Au
Ti
Au
Au
Au

(A)

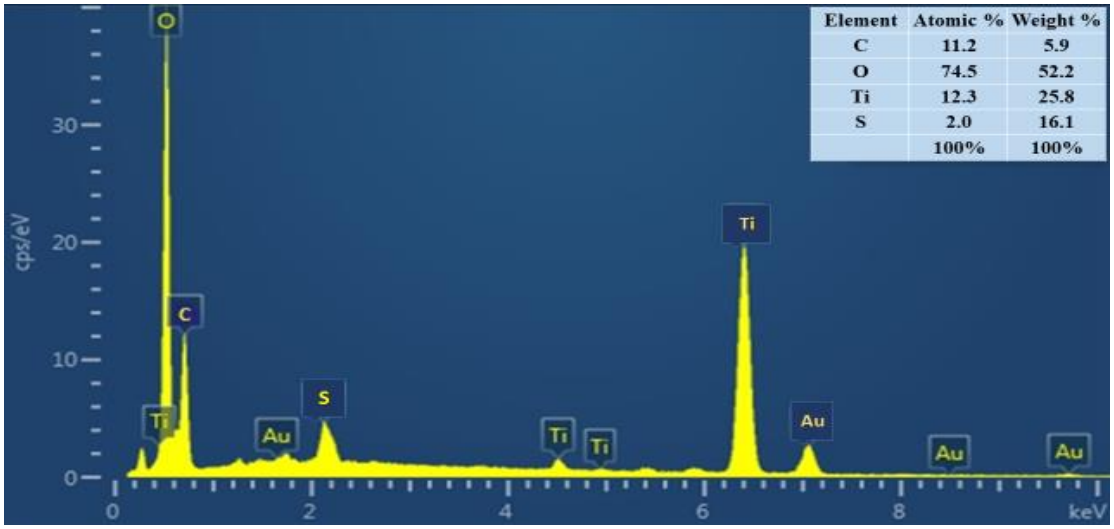
Element Atomic % Weight %
C 11.2 5.9
O 74.5 52.2
Ti 12.3 25.8
S 2.0 16.1
100% 100%
cps/eV
keV
O
C
S
Ti
Au
Ti
Ti
Ti
Au
Au
Au

(B)

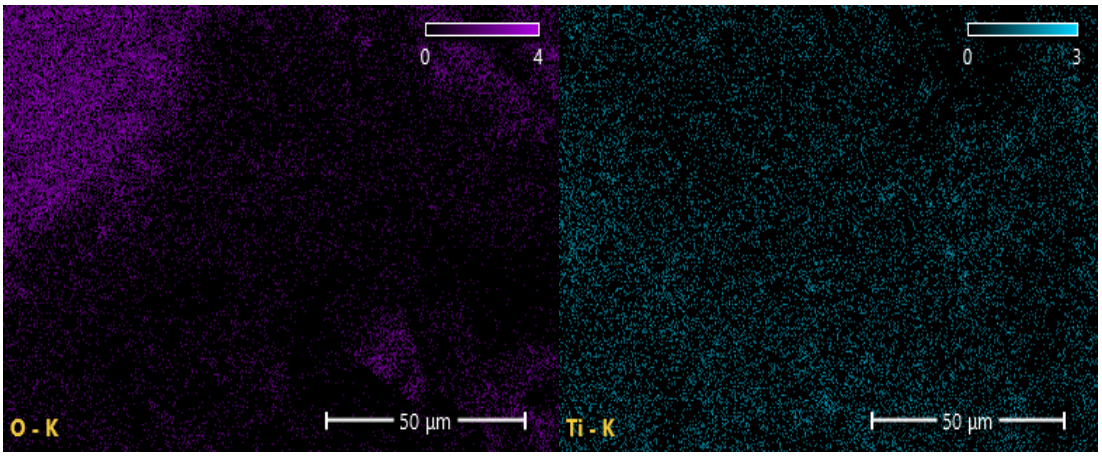
0
4
0
3
O - K
50 µm
Ti - K
50 µm

(C) (D)

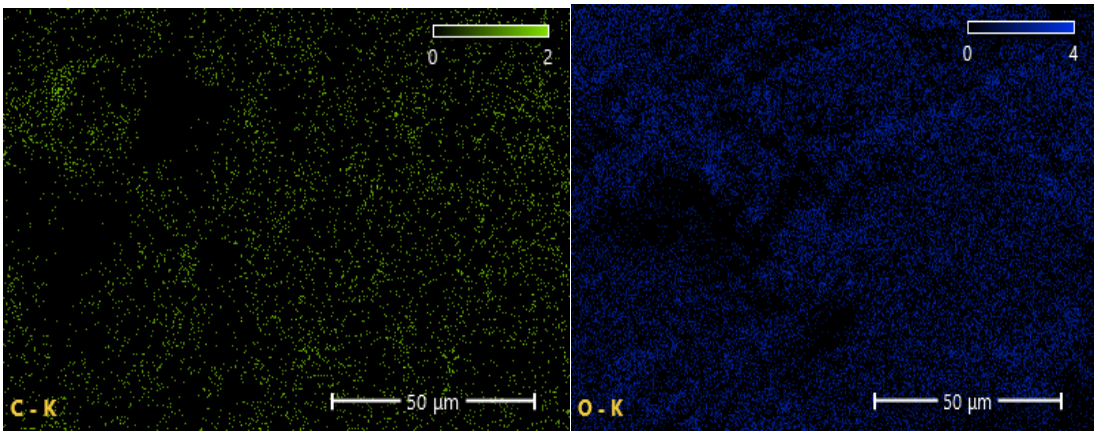

(E) (F)

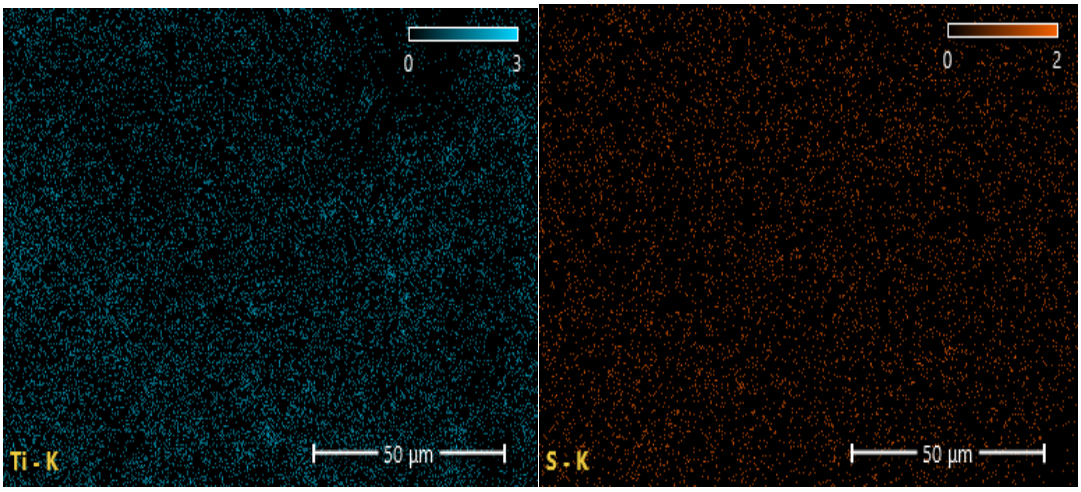

(G) (H)

Fig.5 EDX of **A** TiO_2 NPs, **B** EDX of TiO_2 /Tiopronin prepared by laser ablation, **C,** and **D** mapping images for TiO_2 NPs, **E, F, G**, and **H** mapping images for TiO_2 /Tiopronin nanoparticles.

4.5. TEM of TiO_2 NPs and TiO_2/ Tiopronin nanoparticles

It is evident from the TEM analysis of TiO_2 Nps, which is shown in (Fig. 6 A, B), that the TiO_2 NPs have a narrow size distribution and a quasi-spherical shape with an average diameter of 17 nm. Additionally, the lack of morphological flaws demonstrates the prepared TiO_2 NPs' structural safety and purity. As a result of coating TiO_2 NPs with a layer of Tiopronin with an average diameter of 49 nm, the TiO_2/Tiopronin nanoparticles, which are depicted in (Fig.6 C), clearly appear as a coated sphere as a result of the Tiopronin layer covering. The absence of morphological defects further demonstrates the structural integrity and purity of the prepared TiO_2 NPs.

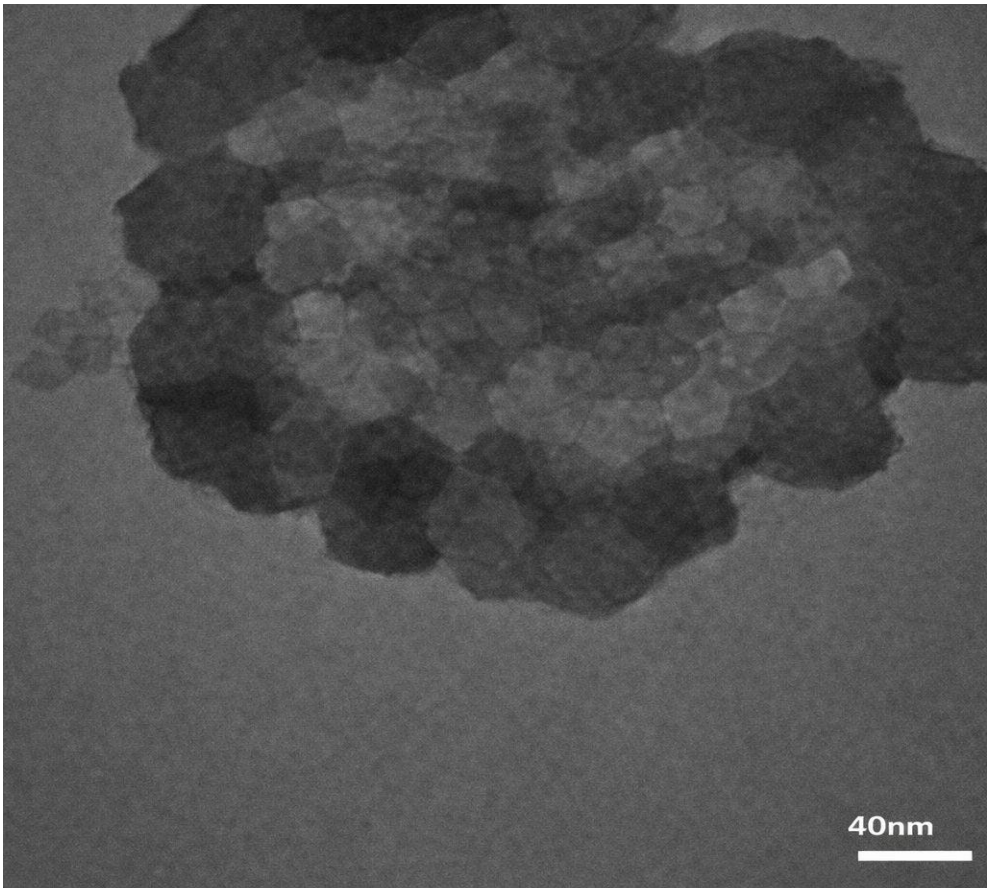

(A)

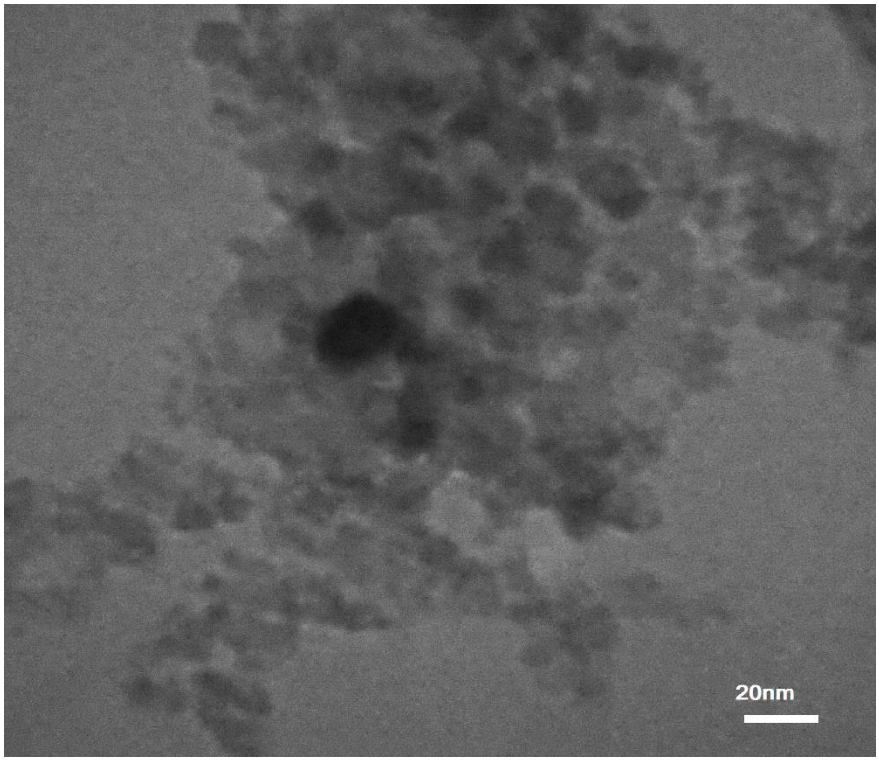

(B)

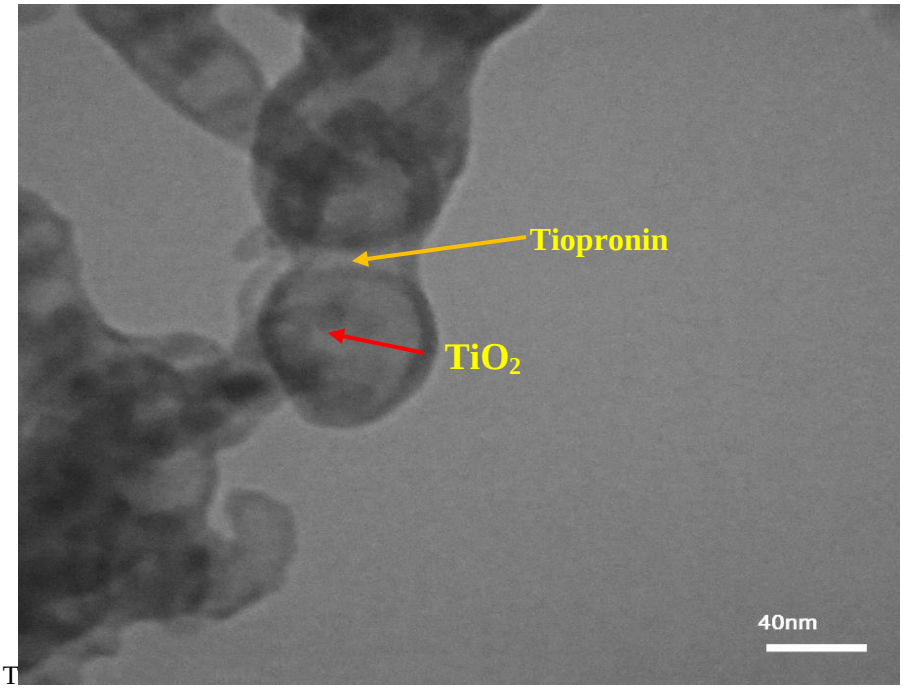

T

(C)

Fig.6 TEM of **A,** and **B** TiO_2 NPs, **C** TEM of TiO_2/Tiopronin nanoparticles prepared by laser ablation.

4.6. Fourier Transform Infrared Spectrophotometer (FTIR) of TiO_2 NPs and TiO_2/ Tiopronin nanoparticles

The FTIR spectrum of pure TiO_2 NPs exhibited a broad and strong absorption band in the 3200–3600 cm^{-1} region as shown in (Fig.7A), attributed to the stretching vibrations of surface hydroxyl groups (O–H) and the physically adsorbed water on the surface. A peak was also observed at approximately 1630 cm^{-1}, attributed to the bending vibrations of the adsorbed water molecules (H–O–H bending). Additionally, a broad and intense absorption band was observed in the 400–800 cm^{-1} region, which is attributed to the vibrations of the Ti–O–Ti and Ti–O bonds. This region serves as a signature for the formation of the titanium oxide structure [24]. The spectrum of Tiopronin exhibited several distinct peaks belonging to organic functional groups as illustrated in the (Fig.7B). A prominent peak appeared at approximately 1754 cm^{-1}, attributed to the C=O stretching vibration of the carboxyl group. Another peak appeared at approximately 1622 cm^{-1}, attributed to the C=O stretching of the amide group. Additional peaks were observed in the 1400–1000 cm^{-1} region, attributed to COO^- symmetric stretching, C–N, and C–O stretching vibrations. A distinctive peak appeared at approximately 2565 cm^{-1}, attributed to the S–H stretching vibration of the thiol group, which is indicative of the presence of Tiopronin [25].

On the other hand, TiO_2 coating with Tiopronin nanoparticles, showed significant changes, including a decrease in the broadband intensity of the O–H signal in the high region of the spectrum as shown in (Fig.7c), This indicates surface coating of the TiO_2 NPs and interaction of the Tiopronin functional groups with the surface hydroxyl sites. Organic peaks were also observed with slight shifts in their positions. The carbonyl peak shifted from approximately 1754 to approximately 1708 cm^{-1}, and the the C=O of the amide group peak shifted from approximately 1622 to approximately 1608 cm^{-1}, suggesting hydrogen bonding or coordination between the Tiopronin groups and the TiO_2 surface [26]. Meanwhile, the broadband intensity attributed to Ti–O–Ti vibrations remained in the low region of the spectrum, confirming that the TiO_2 NPs retained its basic crystalline structure after the coating process. Therefore, the appearance of the characteristic organic peaks of Tiopronin with slight shifts, along with the reduced intensity of the hydroxyl peaks and the persistence of the Ti–O peaks, is clear evidence of the success of the TiO_2 NPs surface coating and modification process using Tiopronin.

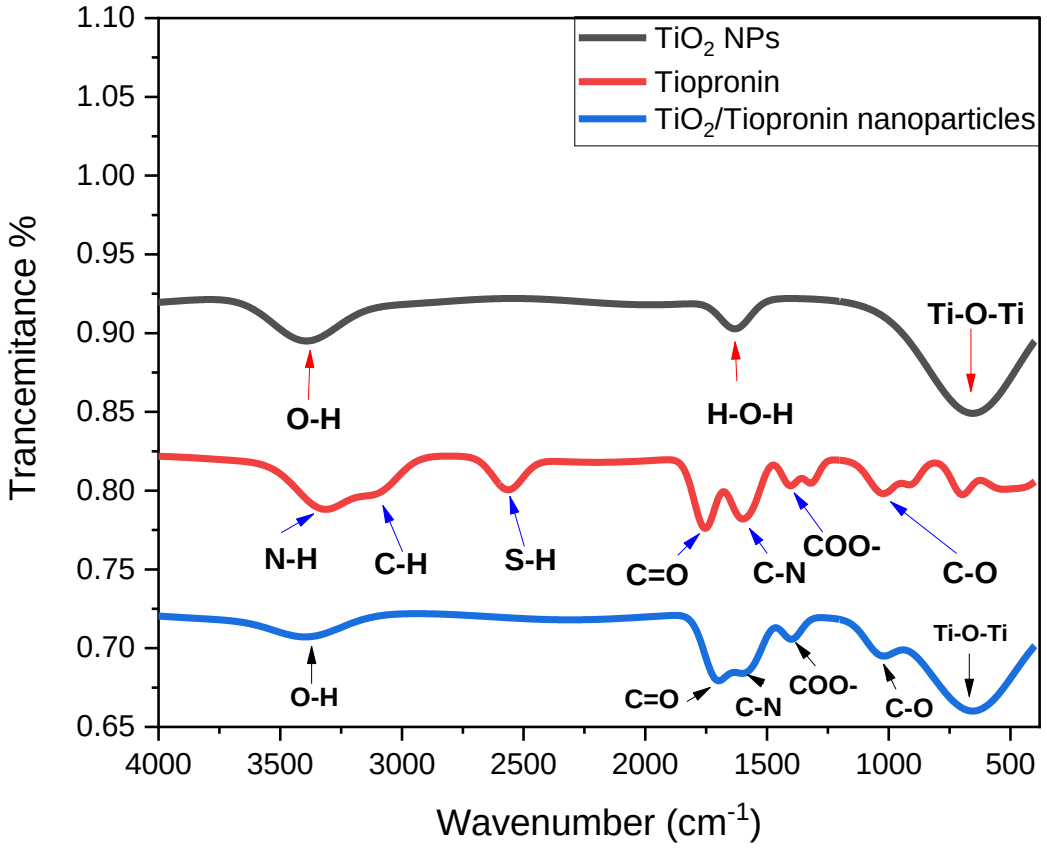

Fig.7 FTIR of **A** TiO_2 NPs, **B** Tiopronin, **c** TiO_2/ Tiopronin nanoparticles

5. Optical properties of TiO_2 NPs and TiO_2/ Tiopronin nanoparticles

UV-Vis spectroscopy is a tool for studying multidisciplinary optical properties and determining electronic energy. TiO_2 NPs exhibit strong optical properties in the UV region at approximately 350 nm, as illustrated in (Fig.8 A), due to a transmission transition from the valence band (VB) to the conduction band (CB). This electronic transition

reflects the semiconducting nature of TiO_2 and yields an energy gap of approximately 3.2 eV, a significant value for the anatase phase of TiO_2, as shown in (Fig.8B).

On the other hand, the optical properties of TiO_2/Tiopronin nanoparticles arise from interactions between organic molecules and the nanomaterial's surface, where Tiopronin contains functional groups such as -SH, -CO, and -NH, capable of binding to the TiO_2 surface, leading to the formation of new energy levels on the material's surface. as a result, more than one absorption peak appears in the 210 nm and 280 nm regions as shown in (Fig.8A), which are attributed to intramolecular electron transfers within the organic molecule, such as $\pi \rightarrow \pi^*$ and $n \rightarrow \pi^*$, and are related to the Tiopronin functional groups [27, 28]. Furthermore, the binding of Tiopronin to the surface of TiO_2 results in a shift towards the larger wavelengths (redshift) in the TiO_2 spectrum. This shift is due to the electronic interaction between the organic molecule and the semiconductor material, resulting in a reduced energy gap from 3.2 eV in TiO_2 that deviates to approximately 2.7 eV in the TiO_2/Tiopronin nanoparticles as shown in (Fig.8B), where a decrease in gap energy indicates a narrowing of the electron gap due to the introduction of surface energy levels or charge transfer between the organic molecule and TiO_2, which leads to an increased ability of the material to absorb light across a wider range of the spectrum. Therefore, the appearance of additional peaks in the spectrum with a decrease in gap energy confirms the successful encapsulation of TiO_2 with Tiopronin and the occurrence of an electronic interaction between the organic compound and the nanoparticle surface, leading to a modification of the material's optical properties [29].

Photoluminescence (PL) spectroscopy is used to study the efficiency of electron-hole pair separation and crystal defects in semiconductor materials. TiO_2 NPs commonly showcase several emission peaks in the violet-inexperienced region of the visible spectrum as illustrated in (Fig.8C) due to electron-hole recombination tactics across one of a kind electricity ranges. For TiO_2 NPs, a main emission peak appears around 380 nm, called near-band-edge emission, as a consequence of the recombination of electrons in the conduction band with holes in the valence band. Another top appears at 490 nm, attributed to emission related to crystal defects, in particular oxygen vacancies or surface defects that act as intermediate power tiers within the electron hole [30]. When TiO_2 is coated with Tiopronin, the photoemission properties change due to the interaction between the organic molecule and the nanoparticle surface. Tiopronin contains functional groups such as -SH, -COOH, and $-NH_2$ that can bind to the TiO_2 surface, creating new surface energy levels that facilitate charge transfer. As a result, emission peaks may appear at approximately 400 nm, 460 nm, and 500 nm as illustrated in (Fig.8C). From (Fig.8C) we can notice a decrease in the intensity of the PL peaks is typically observed when TiO_2 is coated with Tiopronin. This is attributed to the transfer of electrons from TiO_2 to the organic molecule or their retention at surface energy levels, which reduces the rate of electron recombination with holes. This behavior is consistent with the decrease in electron gap energy from 3.2 eV in TiO_2 nanoparticles to approximately 2.7 eV in TiO_2/ Tiopronin nanoparticles where the formation of surface energy levels narrows the electron gap and improves charge separation. Therefore, the decrease in PL emission intensity and the appearance of spectral shifts suggest evidence for the electronic interaction between TiO_2 NPs and Tiopronin and for the successful coating of the nanoparticles, which contributes to modifying the optical properties of the material.

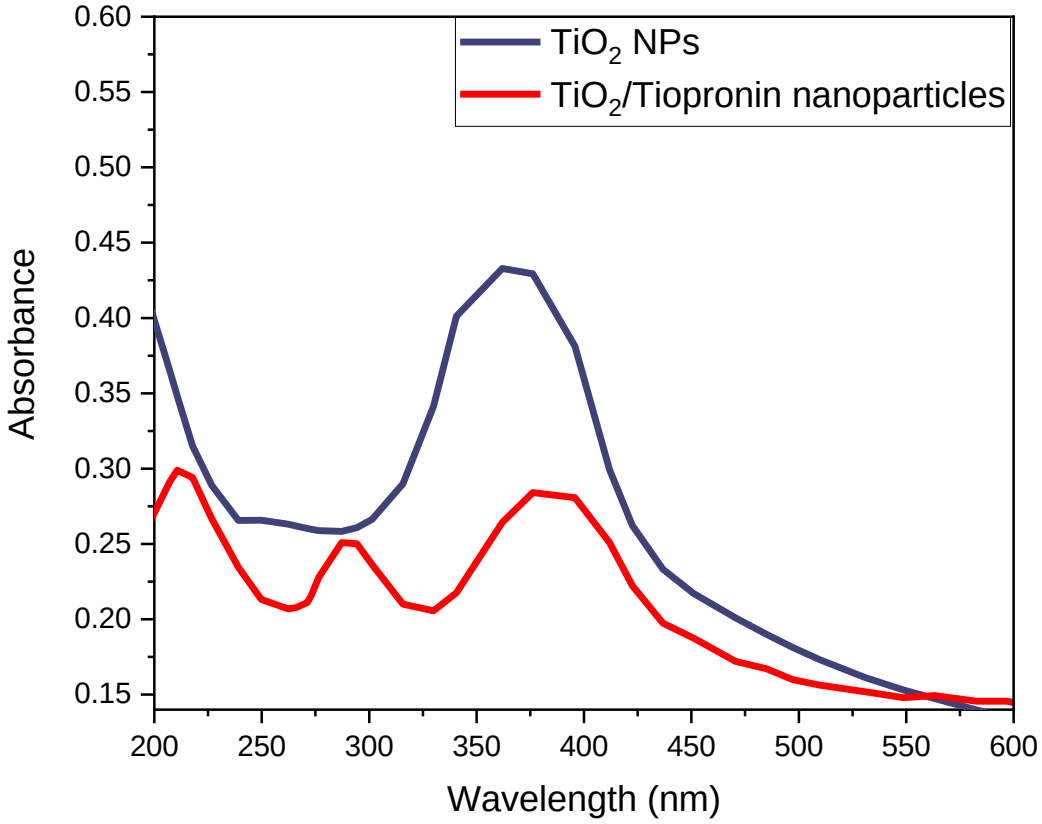
TiO2 NPs
TiO2/Tiopronin nanoparticles
Absorbance
Wavelength (nm)
0.60
0.55
0.50
0.45
0.40
0.35
0.30
0.25
0.20
0.15
200
250
300
350
400
450
500
550
600

(A)

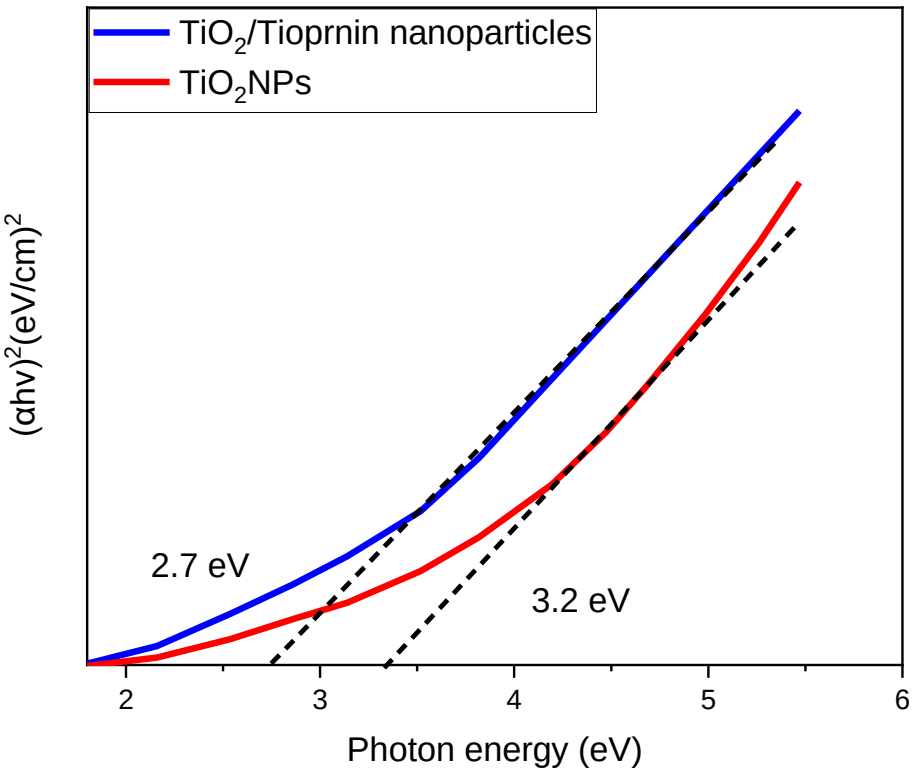
TiO2/Tioprnin nanoparticles
TiO2NPs
(αhv)2(eV/cm)2
Photon energy (eV)
2.7 eV
3.2 eV
2
3
4
5
6

(B)

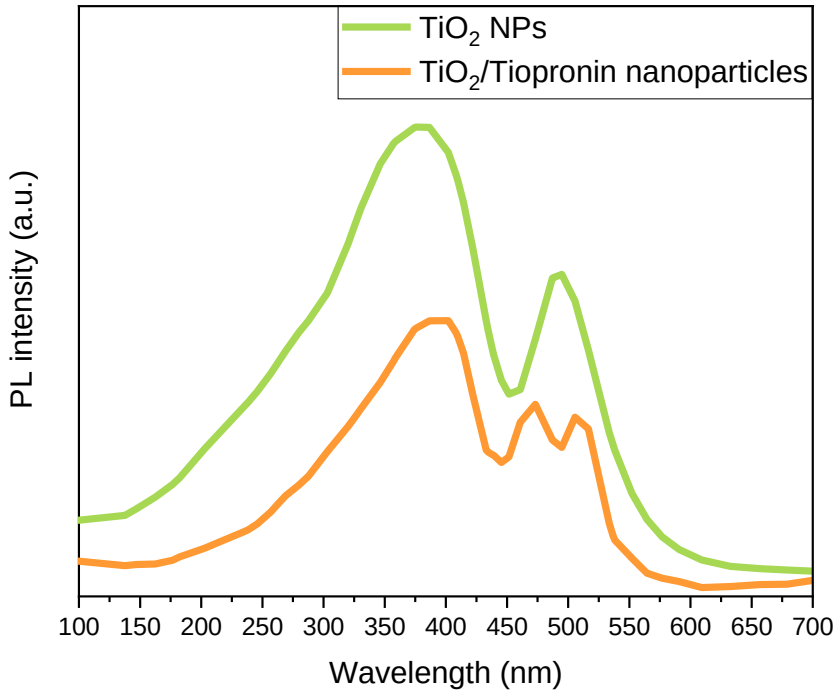

(C)

Fig.8 UV–Vis absorption spectrum of **A** TiO_2 NPs and TiO_2/ Tiopronin nanoparticles, **B** The Tauc plot shows the bandgap energy TiO_2 NPs and TiO_2/ Tiopronin nanoparticles, **C** PL emission spectrum of TiO_2 NPs and TiO_2/ Tiopronin nanoparticles excited at λ_{ex} = 330 nm.

6. Effect of sunlight on *Pseudomonas Aeruginosa* bacteria without nanomaterials

As it is known, ultraviolet rays play an important role in inhibiting the growth of many bacteria that contribute to environmental pollution in one way or another. On this basis, we made a comparison between the effectiveness of ultraviolet rays within sunlight in reducing the speed of the spread of bacteria (*Pseudomonas Aeruginosa*) that causes skin infections and inhibiting Its growth and the effectiveness of using nanomaterials with sunlight in reducing the speed of the spread of bacteria that cause skin infections and discouraging their growth. Through practical application, we noticed that when exposing bacteria of type (*Pseudomonas Aeruginosa*) to sunlight for different periods of time ranging from (1 – 5) hours that sunlight is able to reduce the speed of bacterial spread by up to (32%). In the other word, the remaining bacterial population was 68%, corresponding to an inhibition rate of 32% in just 5 by dispersing the external electrical potential of its membrane and this leads to ending the life of the cell as illustrated in (Fig.9). Nature without disturbing humans and the results can be seen in the (Fig.10) below:

Fig.9 Effect of sunlight on *Pseudomonas Aeruginosa*.

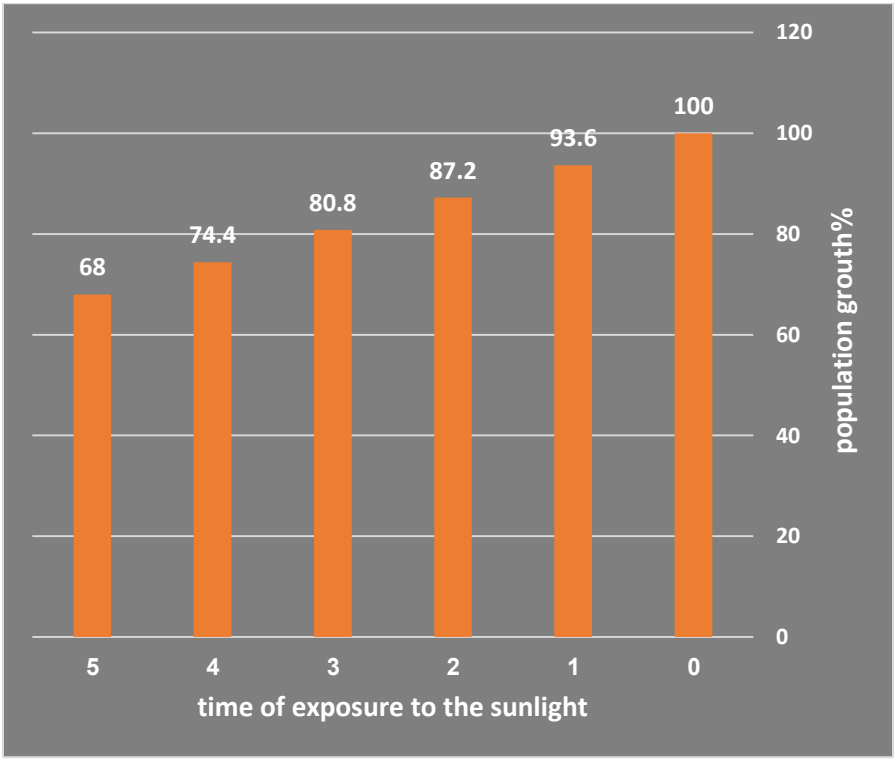

Fig.10 Effect of sunlight on *Pseudomonas Aeruginosa* bacteria without nanomaterials.

7. Effect of TiO_2 NPs and TiO_2/Tiopronin nanoparticles with sunlight on *Pseudomonas Aeruginosa* bacteria

It is known that TiO_2 NPs act as a photocatalyst once exposed to ultraviolet light, and their effectiveness is very high in destroying organic pollutants and in inhibiting the growth of many types of bacteria by forming very strong oxidizing agents which dissipate the external electric potential of the bacterial cell membrane. On this basis, we studied the effect of both uncoated TiO_2 NPs and the effect of a nanoparticles consisting of TiO_2/Tiopronin nanoparticles using (5) different concentrations (0.2 – 1) mg/mL of TiO_2 NPs and TiO_2/Tiopronin nanoparticles for different periods of time (1-5) hours of exposure to natural sunlight to inhibits the growth of bacteria (*Pseudomonas Aeruginosa*) that cause skin infections. Through the practical results, we noticed that there is a very high and unique ability of these TiO_2/Tiopronin nanoparticles and TiO_2 nanoparticles to inhibit the growth of bacterial isolates and thus destroy them. When the concentration of the nanoparticles is 1 mg/mL, it will give the highest inhibition rate up to 90.5% for a period not to exceed (5) hours in the presence of sunlight. In other word, The remaining bacterial population was 9.5%, corresponding to an inhibition rate of 90.5% and this in itself is a unique inhibition by dispersing the external electrical potential of the cell membrane, which leads to Its death, as well as the case of TiO_2 NPs, has also shown an unparalleled success in inhibiting the growth of bacteria(*Pseudomonas Aeruginosa*)), where we noticed that when its concentration is 1 mg / mL and for 5 hours of exposure to sunlight, The remaining bacterial population was 43.5%, corresponding to an inhibition rate of 56.5% , and this is also a new feature added to the features of this distinct nanomaterial , the results can be seen in the (Fig.11), (Fig.12) and (Fig.13 A, B).

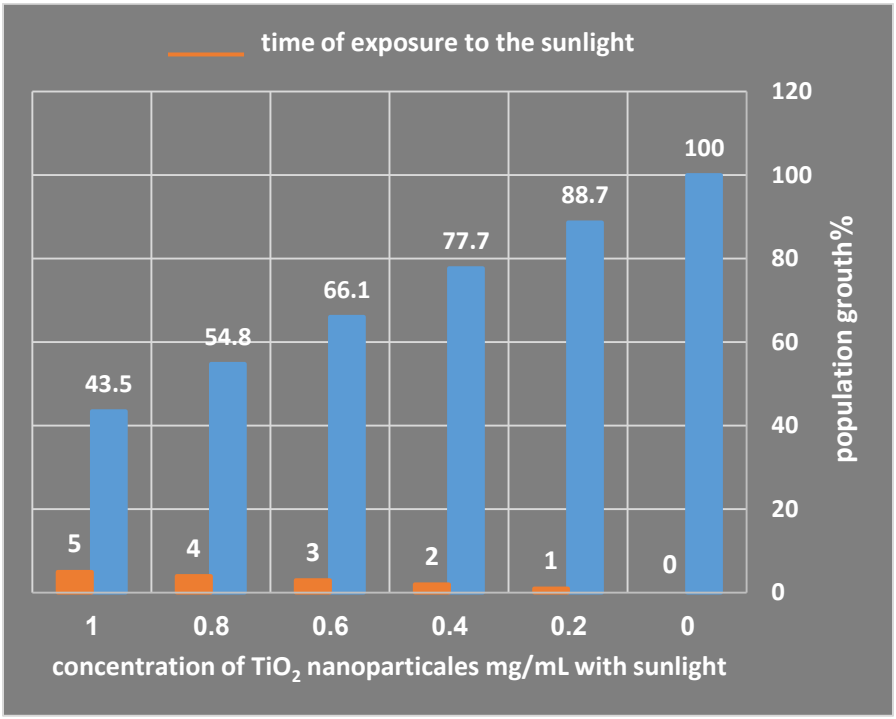

Fig.11 Illustrated the Antibacterial activity of TiO_2 NPs only against *Pseudomonas Aeruginosa*.

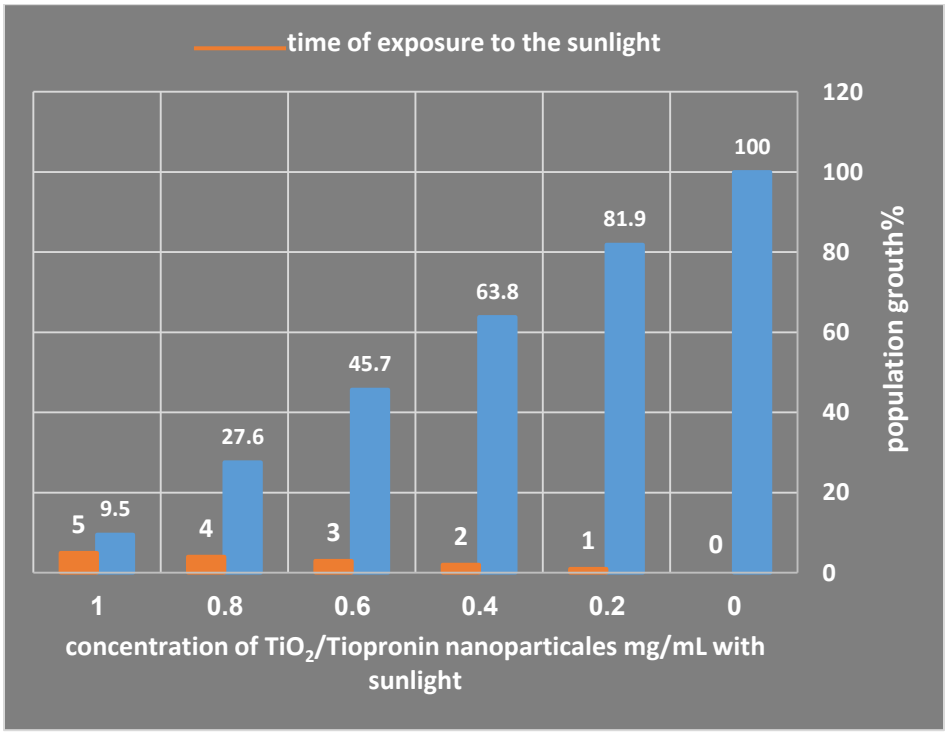

Fig.12 Illustrated the Antibacterial activity of TiO_2/Tiopronin nanoparticles against *Pseudomonas Aeruginosa*.

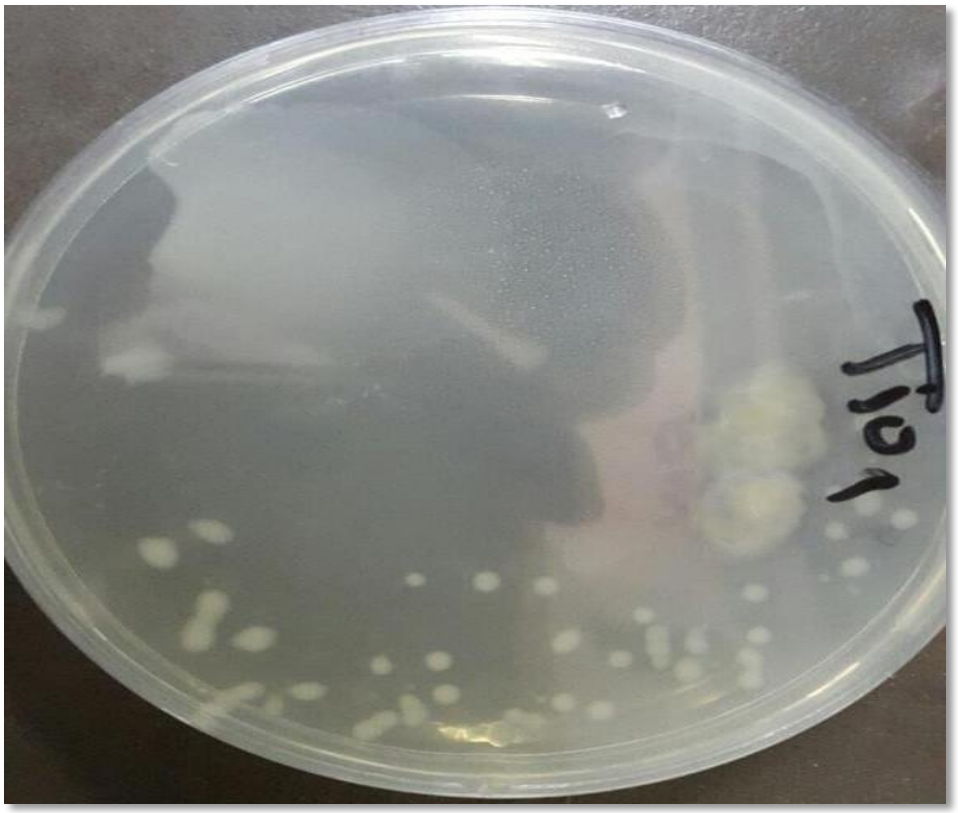

(A)

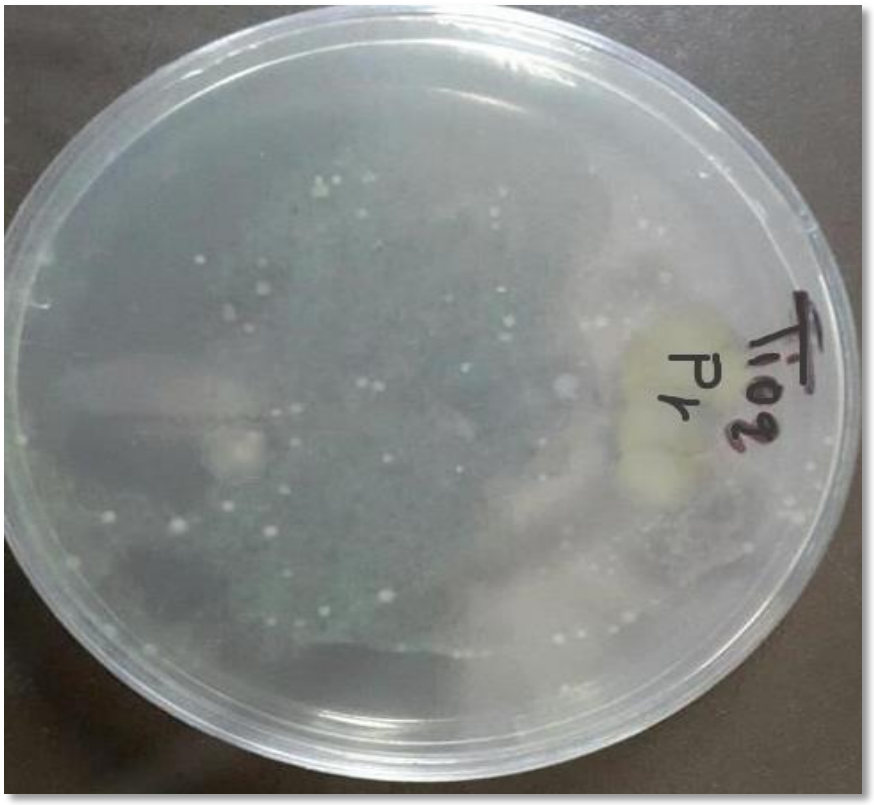

(B)

Fig.13 The Antibacterial activity of **A** TiO_2 NPs only against *Pseudomonas Aeruginosa*, **B** the Antibacterial activity of TiO_2/Tiopronin nanoparticles against *Pseudomonas Aeruginosa.*

8.Comparative antibacterial activity of Tiopronin, TiO_2, and TiO_2/Tiopronin nanoparticles under dark and sunlight conditions against Pseudomonas aeruginosa

The antibacterial activity of Tiopronin, TiO_2 nanoparticles, and TiO_2/Tiopronin hybrid nanoparticles was comparatively evaluated against Pseudomonas aeruginosa under both dark and sunlight irradiation conditions as illustrated in the (Table 3) and (Fig.14). Bacterial suspensions were prepared and divided into seven experimental groups: untreated control, Tiopronin in dark, Tiopronin under sunlight, TiO_2 in dark, TiO_2 under sunlight, TiO_2/Tiopronin in dark, and TiO_2/Tiopronin under sunlight. The concentration of all tested materials was fixed at 1 mg/mL. Samples subjected to irradiation were exposed to sunlight for 5 h, followed by incubation at 37 °C for 24 h. After incubation, serial dilution was performed and aliquots were spread on nutrient agar plates. The number of viable colonies (CFU) was counted and the inhibition percentage was calculated using the following equation (1) [20]. The untreated control exhibited a mean colony depend of two hundred ± 2.0 CFU. Tiopronin remedy in dark situations ended in a mild discount in bacterial increase with a median colony remember of 176 ± 2 Zero CFU, similar to an inhibition efficiency of 12 Zero%. Under sunlight irradiation, Tiopronin confirmed barely more desirable antibacterial activity, reducing the colony count to one hundred sixty ± 2 Zero CFU and attaining 20.0% inhibition. Bare TiO_2 nanoparticles exhibited restrained antibacterial hobby in dark conditions, with an average colony matter of 164 ± 2 Zero CFU and an inhibition performance of 18.0%. However, beneath sunlight irradiation,

TiO_2 nanoparticles confirmed substantially improved antibacterial overall performance, decreasing the feasible remember to 87 ± 2.0 CFU, corresponding to 56.5 % inhibition. The TiO_2/Tiopronin hybrid nanoparticles exhibited superior antibacterial interest in comparison with both character additives. In dark situations, the hybrid machine decreased the colony matter to a hundred and 44 ± 2.0 CFU, reaching 28.0% inhibition. Upon sunlight irradiation, a stated enhancement in antibacterial efficiency become determined, with the colony depend lowering to 19 ± 1.0 CFU and the inhibition performance reaching ninety.5%. These consequences display that daylight irradiation performs a vital function in improving the antibacterial pastime of TiO_2-based totally nanomaterials, even as surface functionalization with Tiopronin in addition improves the overall antibacterial efficiency of the hybrid machine.

Table 3 displays a comparison of the antibacterial activity of Tiopronin, TiO_2 NPs, and TiO_2/Tiopronin hybrid nanoparticles against Pseudomonas aeruginosa in both dark and sunlight-irradiated environments.

Group	Rep1	Rep2	Rep3	Mean_CFU	SD	Inhibition_%
Control	198	200	202	200	2	0
Tiopronin dark	174	176	178	176	2	12
Tiopronin light	158	160	162	160	2	20
TiO_2_dark	162	164	166	164	2	18
TiO_2_light	85	87	89	87	2	56.5
Hybrid_dark	142	144	146	144	2	28
Hybrid_light	18	19	20	19	1	90.5

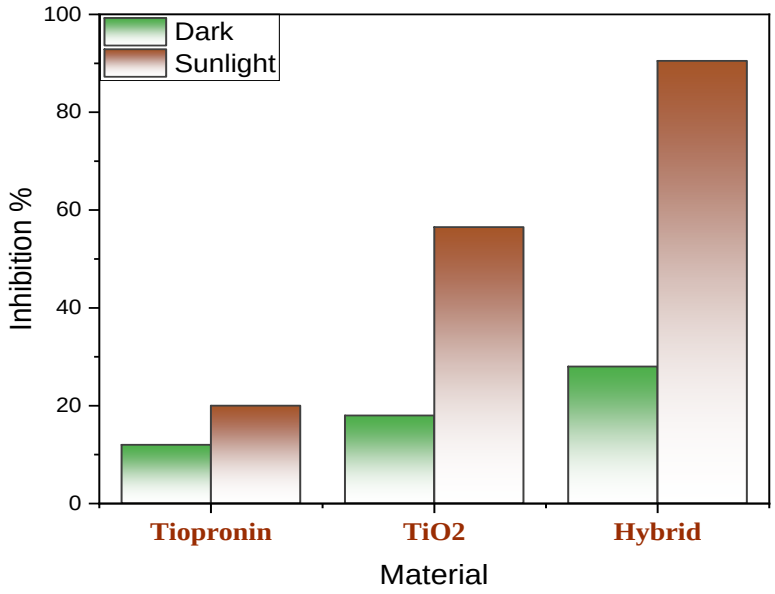

Fig.14 The antibacterial activity of Tiopronin, TiO_2 NPs, and TiO_2/Tiopronin hybrid nanoparticles against *Pseudomonas aeruginosa* in both dark and sunlight-irradiated environments.

8. Reactive oxygen species (ROS) scavenger test

To identify the main reactive oxygen species responsible for the antibacterial activity of TiO_2/Tiopronin nanoparticles, scavenger trapping experiments were performed under the same antibacterial conditions as illustrated in (Fig.15). Pseudomonas aeruginosa suspensions were treated with TiO_2/Tiopronin nanoparticles at a concentration of 1 mg/mL. Specific scavengers were added separately, including isopropanol (10 mM) for hydroxyl radicals (•OH), p-benzoquinone (1 mM) for superoxide radicals (O_2•$^-$), and EDTA (1 mM) for photogenerated holes (h^+). The mixtures were kept in the dark for 10 min, then exposed to sunlight for 5 h, followed by incubation at 37 °C for 24 h. After incubation, serial dilution and CFU counting were performed, and the inhibition percentage was calculated. Control groups containing bacteria with scavenger only were also included. The antibacterial efficiency of TiO_2/Tiopronin nanoparticles decreased in the presence of different scavengers, confirming the involvement of reactive oxygen species in the bacterial inactivation mechanism. The most extensive discount in inhibition became discovered after including isopropanol, indicating that hydroxyl radicals (•OH) were the dominant reactive species. A mild lower became determined inside the presence of p-benzoquinone, suggesting a secondary contribution of superoxide radicals (O_2•$^-$). In assessment, the effect of EDTA was much less reported, indicating a lower contribution of photogenerated holes (h^+). These consequences exhibit that the enhanced antibacterial interest of the hybrid nanoparticles underneath daylight is specifically governed with the aid of photocatalytic ROS technology, particularly hydroxyl radicals.

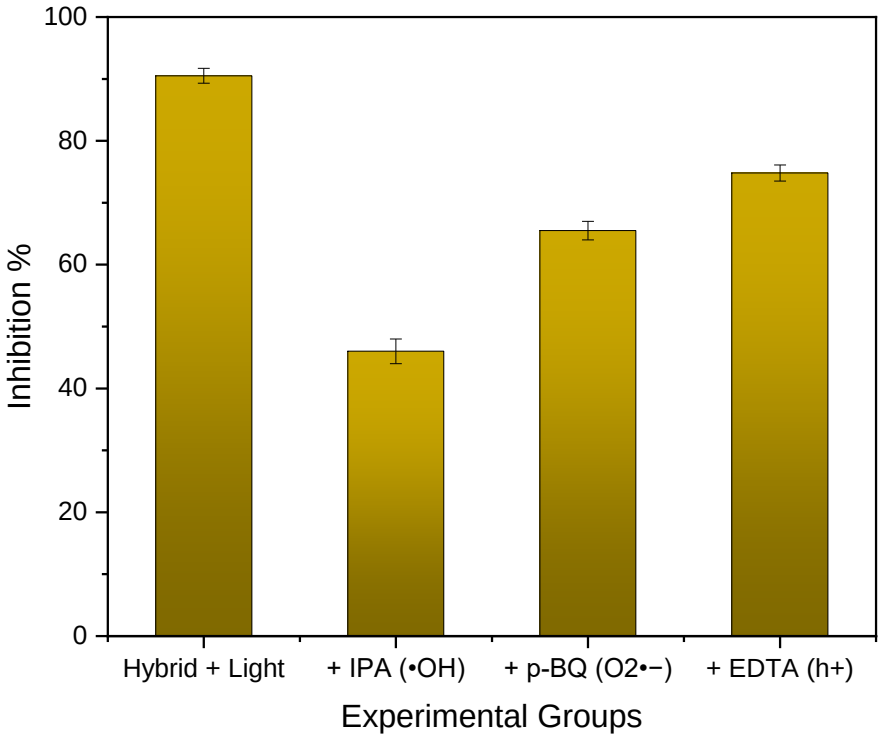

Fig.15 (ROS) scavenger test.

9. TiO_2/Tiopronin nanoparticles mechanism for inhibiting *Pseudomonas Aeruginosa* activity

The antibacterial activity of TiO_2 NPs coated with Tiopronin relies on the synergy of several physical and chemical mechanisms that enhance photocatalytic activity and surface interaction with bacterial cells. When TiO_2 NPs are exposed to light radiation with an energy equal to or greater than the electron hole energy, electrons move from the valence band to the conduction band, forming electron-hole pairs. These pairs then participate in redox reactions with oxygen and water, generating reactive oxygen species, including hydroxyl radicals (•OH), peroxides (H_2O_2), superoxide anions ($O_2•^-$), and hydroperoxyl radicals ($HO_2•$). These species possess a high oxidative capacity, leading to the oxidation of lipids comprising the bacterial cell membrane, damage to proteins and enzymes, and harm to genetic material. This results in loss of cell membrane integrity, increased permeability, and leakage of cellular components. When TiO_2 particles are coated with taypronine, which contains active functional groups such as -SH, -COOH, and $-NH_2$, the molecule binds to the TiO_2 surface, forming an organic layer that acts as a stabilizing agent. This prevents the nanoparticles from clumping together and improves their dispersion in the medium, thus increasing the effective surface area and direct contact with bacterial cells as shown in (Fig.16). Furthermore, the sulfur groups in Tiopronin can act as electron-capturing sites, reducing electron and hole recombination and extending the lifetime of generated charges, thereby increasing the efficiency of reactive oxygen species generation. Furthermore, the thiol group (-SH) can directly interact with bacterial proteins, particularly disulfide bonds in enzymes and membrane proteins, altering their structure and disrupting their vital activity. This leads to the disruption of essential processes such as cellular respiration, electron transport, and increased cell membrane permeability. The synergy between increased generation of reactive oxygen species, enhanced nanoparticle dispersion, and the direct interaction between thiol groups and bacterial cell protein components ultimately promotes intracellular oxidative stress, inhibiting bacterial growth or eliminating the bacteria.

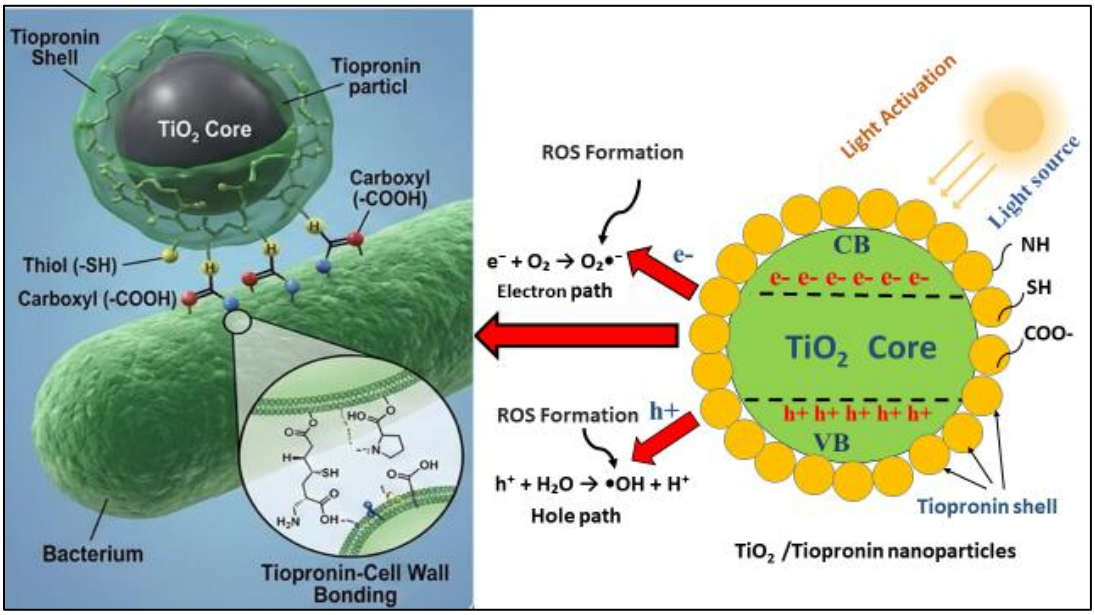

Fig.16 Chemical mechanism for inhibiting bacterial activity using TiO_2/Tiopronin nanoparticles.

10. Comparing with previous research

The results of our study were compared with those of other previous studies that used the TiO_2 NPs to inhibit the growth of different bacteria [3, 10, 12, 31, 32], as shown in (Table 4).

Table 4. displays a comparison between this study and some earlier Bacterial inhibition research using TiO_2 NPs.

NO.	Nanomaterial	Dose of Nanomaterial	Synthesis method	Bacterial type	% inhibition	Reference
1-	TiO_2 NPs	50-100 µg/mL	Laser ablation in liquid (LAL) in ethanol solution	*Gram-Negative*	60-70%	3
2-	TiO_2 NPs	150 µg/mL	Laser ablation in liquid (LAL)	*Gram-Negative*	75%	10
3-	TiO_2 NPs	100 µg/mL	Laser ablation in liquid (LAL) in water	*P.aeruginosa*	70-80%	12
4-	TiO_2 NPs	200 µg/mL	Sol-gel	*E.Coli*	65-75%	31
5-	TiO_2 Nanotubes	__	Electrochemical synthesis (Anodization)	Mixed	80-85%	32
6-	TiO_2 NPs + sunlight	0.2-1 mg/mL	Laser ablation in liquid (LAL) in ethanol: acetic acid	*Pseudomonas Aeruginosa*	56.5%	This work
7-	TiO_2/Tiopronin + sunlight	0.2-1 mg/mL	Laser ablation in liquid (LAL) in ethanol: acetic acid	*Pseudomonas Aeruginosa*	90.5%	This work
8-	Sunlight only without nanomaterials	_____	_____	*Pseudomonas Aeruginosa*	32%	This work

Conclusion

In this study, an organic-inorganic hybrid nanostructure composed of TiO_2 NPs and TiO_2/Tiopronin nanoparticles was prepared using liquid laser ablation (LAL), a clean and environmentally friendly method. Structural analyses revealed the formation of highly pure crystalline TiO_2 NPs from the anatase phase with an average crystal size of 20 nm, while the TiO_2/Tiopronin nanoparticles exhibited a relatively larger size 53 nm due to the formation of an organic coating on the particle surface. FE-SEM and TEM analyses revealed quasi-spherical particles with a similar

size distribution, confirming the successful encapsulation of the TiO_2 NPs with the Tiopronin. Optical studies revealed a significant modification in the electronic structure of the material after Tiopronin coating. The energy gap decreased from 3.2 eV in pure TiO_2 NPs to 2.7 eV in TiO_2/Tiopronin nanoparticles, accompanied by a shift in absorption spectra and a decrease in photoluminescence intensity. These consequences indicate progressed electron-gap pair separation and the emergence of extra surface power degrees due to the interaction between TiO_2 and the Tiopronin useful businesses. Bacterial checking out additionally validated that the TiO_2/Tiopronin hybrid nanoparticles exhibited substantially higher inhibitory interest in opposition to Pseudomonas aeruginosa in comparison to natural TiO_2 NPs or daylight by myself. When uncovered to daylight at attention of one mg/mL, the TiO_2/Tiopronin nanoparticles achieved 90.5% bacterial inhibition, even as natural TiO_2 NPs done most effective approximately 56.5 %, and sunlight on my own did no longer exceed 32%. This more suitable antibacterial activity is attributed to the synergistic impact of photocatalytic reactive oxygen species (ROS) era, progressed nanoparticle dispersion, reduced electron and hollow recombination quotes, and the direct interplay among the thiol companies in Tiopronin and proteins in bacterial cells. Overall, the results display that the TiO_2/Tiopronin hybrid nanoparticles prepared using laser ablation constitute a promising nanomaterial with stronger antibacterial activity and optical performance. This method additionally affords a simple, low-price, and environmentally pleasant pathway for generating practical nanomaterials that would have important future programs in biomedical fields, especially in antimicrobial surfaces and the treatment of burn wound infections.

Declarations

Ethical Approval

Not applicable.

Funding

The authors received no specific funding for this work.

Data Availability Statement

Data available on request from the author.

Conflicts of Interest

The authors declare that there are no conflicts of interest.

Acknowledgment

The authors thank their institution (Mustansiriyah University) for its continued facilities.

References

[1] Gebre SH, Sendeku MG (2019) New frontiers in the biosynthesis of metal oxide nanoparticles and their environmental applications: an overview. SN Appl Sci 1:1–28. https://doi.org/10.1007/s42452-019-0931-4

[2] Azar BE, Ramazani A, Fardood ST, Morsali A (2020) Green synthesis and characterization of $ZnAl_2O_4$@ZnO nanoparticles and its environmental applications in rapid dye degradation. Optik 208:164129. https://doi.org/10.1016/j.ijleo.2019.164129

[3] Aziz WJ, Ali SQ, Jassim NZ (2018) Production TiO_2 nanoparticles using laser ablation in ethanol. Silicon 10:2101–2107. https://doi.org/10.1007/s12633-017-9612-9

[4] Nabi G, Raza W, Tahir MB (2020) Green synthesis of TiO_2 nanoparticle using cinnamon powder extract and the study of optical properties. J Inorg Organomet Polym Mater 30:1425–1429. https://doi.org/10.1007/s10904-019-01248-3

[5] Arularasu MV (2019) Effect of organic capping agents on the optical and photocatalytic activity of mesoporous TiO_2 nanoparticles by sol–gel method. SN Appl Sci 1:393. https://doi.org/10.1007/s42452-019-0424-5

[6] Hamza RZ, Gobouri AA, Al-Yasi HM, Al-Talhi TA, El-Megharbel SM (2021) A new sterilization strategy using TiO_2 nanotubes for production of free radicals that eliminate viruses and application of a treatment strategy to combat infections caused by emerging SARS-CoV-2 during the COVID-19 pandemic. Coatings 11:680. https://doi.org/10.3390/coatings11060680

[7] Ruddaraju LK, Pammi SVN, Guntuku SG, Padavala VS, Kolapalli VRM (2020) A review on anti-bacterials to combat resistance: From ancient era of plants and metals to present and future perspectives of green nanotechnological combinations. Asian J Pharm Sci 15:42–59. https://doi.org/10.1016/j.ajps.2019.03.002

[8] Alsheheri SZ (2021) Nanoparticles containing TiO_2 for environmental remediation. Des Monomers Polym 24:22–45. https://doi.org/10.1080/15685551.2021.1876322

[9] Honarmand MM, Mehr ME, Yarahmadi M, Siadati MH (2019) Effects of different surfactants on morphology of TiO_2 and Zr-doped TiO_2 nanoparticles and their applications in MB dye photocatalytic degradation. SN Appl Sci 1:1–12. https://doi.org/10.1007/s42452-019-0522-4

[10] Bahjat HH, Ismail RA, Sulaiman GM, Jabir MS (2021) Magnetic field-assisted laser ablation of TiO_2 nanoparticles in water for antibacterial applications. J Inorg Organomet Polym Mater:1–8. https://doi.org/10.1007/s10904-021-02051-4

[11] Khairani IY, Mínguez-Vega G, Doñate-Buendía C, Gökce B (2023) Green nanoparticle synthesis at scale: A perspective on overcoming the limits of pulsed laser ablation in liquids for high-throughput production. Phys Chem Chem Phys. https://doi.org/10.1039/D3CP01214J

[12] Khashan KS, Sulaiman GM, Abdulameer FA, Albukhaty S, Ibrahem MA, Al-Muhimeed T, AlObaid AA (2021) Antibacterial activity of TiO_2 nanoparticles prepared by one-step laser ablation in liquid. Appl Sci 11:4623. https://doi.org/10.3390/app11104623

[13] Haleem A, Mohammed H, Ahmed R (2018) Green synthesis, characterization and antimicrobial activity of TiO_2 nanoparticles using laser ablation technique. Eng Technol J 36:23–29. https://doi.org/10.30684/etj.36.1C.3

[14] Dell'Aglio M, De Giacomo A, Gaudiuso R, De Pascale O (2014) Photocatalytic and antibacterial activity of TiO_2 nanoparticles obtained by laser ablation in water. Appl Catal B Environ 148–149:144–152. https://doi.org/10.1016/j.apcatb.2014.10.031

[15] Haji SH, Mahmood AA, Ibrahim KM (2024) Enhanced antibacterial and antibiofilm properties of TiO_2 nanoparticles biosynthesized by multidrug-resistant Pseudomonas aeruginosa. BMC Microbiol 24:1–15. https://doi.org/10.1186/s12866-024-03530-y

[16] Faisal M, Ismail AA, Al-Sayari SA (2020) Antibacterial activity of TiO_2-doped ZnO composite synthesized via laser ablation route. J Mater Res Technol 9:10223–10231. https://doi.org/10.1016/j.jmrt.2020.05.103

[17] Kumar A, Estes Bright LM, Garren MRS, Manuel J, Shome A, Handa H (2023) Chemical modification of Tiopronin for dual management of cystinuria and associated bacterial infections. ACS Appl Mater Interfaces 15:43332–43344. https://doi.org/10.1021/acsami.3c07160

[18] Mahmood RS, Hussain DH, Aboud NAA (2025) Green laser-ablated CdS nanoparticles in aloe vera medium: structural, optical, electrochemical, and synergistic photocatalytic–adsorptive performance for pentachlorophenol degradation. J Mater Sci Mater Electron 36:2135. https://doi.org/10.1007/s10854-025-16253-1

[19] Modersitzki F, Goldfarb DS, Goldstein RL, Sur RL, Penniston KL (2019) Assessment of health-related quality of life in patients with cystinuria on Tiopronin therapy. Urolithiasis:1–8.

[20] Alt V, Bechert T, Steinrücke P, Wagener M, Seidel P, Dingeldein E, Domann E, Schnettler R (2013) Silver-Tiopronin nanoparticles embedded in bone cement provide antibacterial activity against MRSA. Int J Nanomedicine 8:1791–1801. https://doi.org/10.2147/IJN.S42822

[21] Panáček A, Kvítek L, Prucek R, Kolář M, Večeřová R, Pizúrová N, Sharma VK, Nevěčná T, Zbořil R (2006) Silver colloid nanoparticles: synthesis, characterization, and their antibacterial activity. J Phys Chem B 110:16248–16253.https://doi.org/10.1021/jp063826h

[22] Sellami H, Akinyemi MO, Gdoura-Ben Amor M, Onwudiwe DC, Mthiyane D (2025) Structural and optical characterization of TiO_2 nanoparticles synthesized using Globularia alypum leaf extract and the antibacterial properties. SN Appl Sci 7:1–19. https://doi.org/10.1007/s42452-025-07521-0

[23] Mahmood RS, Mahmood YT, Rheima AM, Aboud NAA (2026) Thermodynamic and kinetic studies of photochemically produced Co_3O_4 nanoparticles for the adsorption of pentachlorophenol pesticide from irrigation water. J Nanotechnol 2026:1–12. https://doi.org/10.1155/jnt/9542499

[24] Nakamoto K (2009) Infrared and Raman spectra of inorganic and coordination compounds, 6th edn. Wiley. https://doi.org/10.1002/9780470405840

[25] Silverstein RM, Webster FX, Kiemle DJ (2005) Spectrometric identification of organic compounds, 7th edn. Wiley.

[26] Coates J (2000) Interpretation of infrared spectra, a practical approach. In: Meyers RA (ed) Encyclopedia of analytical chemistry. John Wiley & Sons. https://doi.org/10.1002/9780470027318.a5606

[27] Li X, Wang J, Zhang Y, Zhao Y (2017) Electronic properties of TiO_2-based materials characterized by high Ti^{3+} self-doping and low recombination rate of electron–hole pairs. RSC Adv 7:12163–12170. https://doi.org/10.1039/C6RA27111A

[28] Zhang H, Chen G, Bahnemann DW (2011) Improved visible light photocatalytic activity of titania doped with tin and nitrogen. J Mater Chem 21:325–331. https://doi.org/10.1039/C0JM02539A

[29] Fujishima A, Zhang X, Tryk DA (2008) TiO_2 photocatalysis: present situation and future approaches. Surf Sci Rep 63:515–582. https://doi.org/10.1016/j.surfrep.2008.10.001

[30] Chen X, Mao SS (2007) TiO_2 nanomaterials: synthesis, properties, modifications, and applications. Chem Rev 107:2891–2959. https://doi.org/10.1021/cr0500535

[31] Arularasu MW, Dhanapandian S, Ramasamy R (2019) Synthesis and characterization of TiO_2 nanoparticles by sol-gel method. SN Appl Sci 1:1275.https://doi.org/10.1007/s42452-019-1275-5

[32] Hamza MS, Al-Hashimi AM (2021) Evaluation of antibacterial activity of TiO_2 nanotubes. Coatings 11:950. https://doi.org/10.3390/coatings11080950